LAWRENCE
LIVERMORE
NATIONAL
LABORATORY

LLNL-TR-419842

Report on Ultra-high Resolution Gamma- / X-ray Analysis of Uranium Skull Oxide

Stephan Friedrich, Miguel Velazquez, Owen Drury, Salem Salaymeh

November 9, 2009

Disclaimer

This work performed under the auspices of the U.S. Department of Energy by Lawrence Livermore National Laboratory under Contract DE-AC52-07NA27344.

Report on Ultra-high Resolution γ- / X-ray Analysis of Uranium Skull Oxide

Team: Stephan Friedrich, Miguel Velazquez, Owen Drury (LLNL)
Saleem Salaymeh (SRNL)

Abstract: We have utilized the high energy resolution and high peak-to-background ratio of superconducting TES γ-detectors at very low energies for non-destructive analysis of a skull oxide derived from reprocessed nuclear fuel. Specifically, we demonstrate that superconducting detectors can separate and analyze the strong actinide emission lines in the spectral region below 60 keV that are often obscured in γ-measurements with conventional Ge detectors.

Sample: We obtained a solution of a highly enriched uranium samples from Y-12 containing uranium fuel "skull oxide", a term that refers to metal fragments from a casting process that have been oxidized in the furnace used for the casting process. The skull oxide uranium material was described by Y-12 as approximately 91% U-235, with 2% U-233. ICP-MS at SRNL showed an atomic composition of:

U-233	1.59%
U-234	0.83%
U-235	89.99%
U-236	0.43%
U-238	7.08%

A 0.05 ml aliquot of the solution was pipetted onto small platinum planchets, evaporated to dryness under a heat lamp and placed into a flame from a propane Bunsen burner until the activity had fused into the platinum and thus been fixed onto the planchets. The samples were analyzed at SRNL with a 20-mm thick, 2000 mm^2 area semi-planar HPGe detector to observe the low energy γ-/X-ray spectra. The samples were then assayed using nominally 40% efficient coaxial HPGe detectors (figure 1) and α analysis.

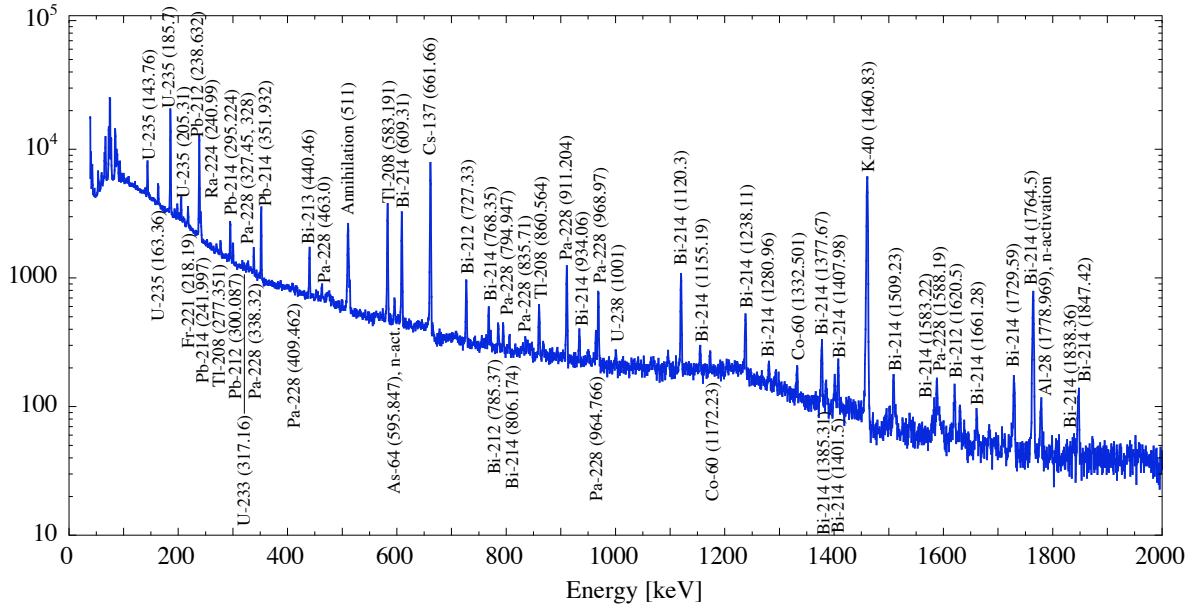

Figure 1: Gamma spectrum of the skull oxide taken with a coaxial high-purity Ge detector.

The spectrum shows emission lines from the actinide in the sample and typical background radioactivity from K-40, Bi-212 and Bi-214, Tl-208. The fission product Cs-137 (662 keV) and the activation product Co-60 (lines at 1172 and 1332 keV) illustrate that the skull oxide contains reprocessed materials. The measured activities in a 0.05 ml sample (including background activity) are:

Radionuclide	Activity (dpm±1σ)
Tl-208	6.30E+03 ± 10%
Bi-212	2.06E+04 ± 10%
Pb-212	1.96E+04 ± 10%
Ra-224	1.96E+04 ± 10%
U-235	2.43E+04 ± 10%
Pu-238	9.20E+05 ± 10%
Am-241	1.95E+03 ± 30%
Pu-239/240	1.55E+04 ± 20%

For comparison with the superconducting spectrometer whose energy range extends to roughly ~200 keV, figure 2 shows the low-energy γ-spectrum of the skull oxide. Emission lines from the fissile uranium isotopes U-233 and U-235 are visible, while the plutonium emission lines are too weak to be detectable above the Compton background of the high-energy radiation. The assignment of the line at 99.85 keV to Pu-238 is somewhat uncertain, given that the stronger Pu-238 line at 43.5 keV is not visible although the Compton background is lower in that energy range and there are no overlapping lines. It could also be due to Ac-225, a daughter of U-233 and Th-229, given that the short-lived Fr-221 (218.19 keV) and Bi-213 (440.46 keV) isotopes further down the decay chain are also detected. The strong actinide L X-rays below 20 keV cannot be fully resolved. The Pt planchet that the sample is fused into produces secondary Pt X-rays, and the Pb shielding (which contains small amounts of In) accounts for the Pb X-rays between 70 and 85 keV as well as for the In Kα1 line at 24.21 keV. Background neutron activation of the detector material produces the Ge-75m line at 139 keV and the As-71 line at 175 keV.

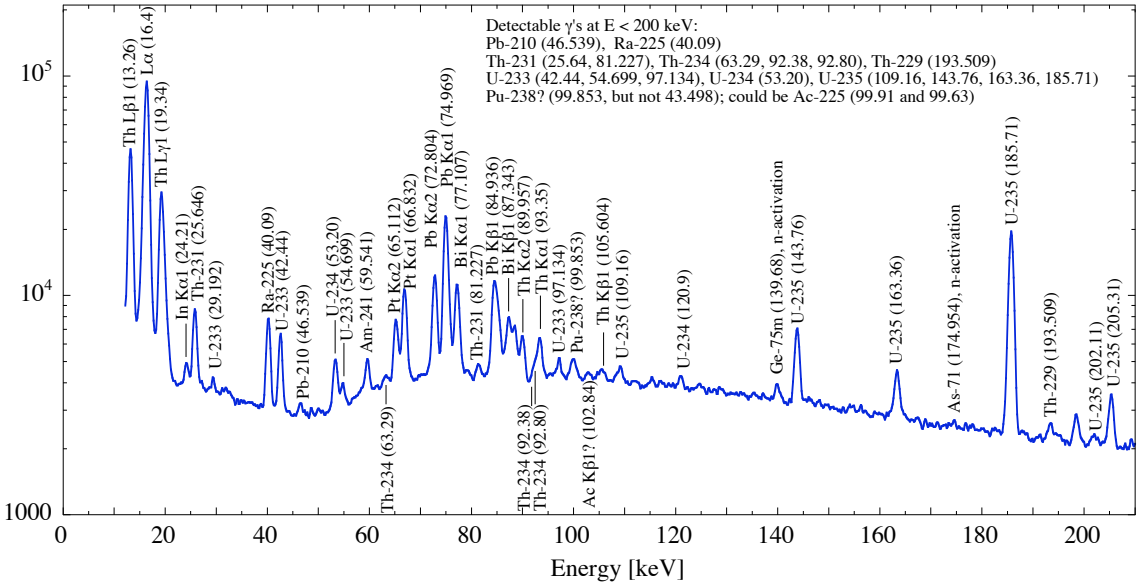

Figure 1: Low-energy HPGe γ-spectrum of the skull oxide on a Pt planchet surrounded by Pb shielding.

LLNL setup: The samples were analyzed at LLNL with a superconducting Mo/Cu transition edge sensor (TES) with a 1 × 1 × 0.5 mm^3 thick Sn γ-absorber. The cryostat temperature was regulated at 90 mK, and the detector was voltage biased at the bottom of the superconducting-to-normal transition. Gamma-induced pulses were read out with a SQUID pre-amplifier and optimally filtered off-line. Since the total activity of the skull oxide sample is low and the active area of the superconducting detector pixel is only ~1 mm^2, the data acquisition rate was only 0.5 counts/s. Several 6-hour runs were therefore taken to improve statistics. The detector resolution varied between ~140 eV and ~160 eV FWHM. However, small drifts in the detector response over time degrade the resolution of the combined spectrum to ~180 eV FWHM and cause a non-Gaussian component in the line shape. Still, the resolution is ~4× better than for Ge detectors and sufficient to resolve the different low-energy lines in the spectrum, e.g. to separate U L X-rays from the decay of the Pu isotopes and the Th L X-rays that accompany the decay of the U isotopes in the sample (figure 3).

The spectrum was calibrated using Th $L_{\alpha 1}$ X-rays at 12.968 keV, the Th $L_{\beta 1}$ line 16.202 keV and the Th $L_{\gamma 1}$ line at 18.98 keV. However, the literature values for low-energy X-ray and γ-ray energies can vary by ±100 eV (!) and thus introduce large systematic calibration errors. For example, even the energy of the strong Th $L_{\alpha 1}$ line is listed at 13.0 keV in the Brookhaven ENDL data base, and at 12.968 keV at the LBNL table of isotopes, and the U $L_{\beta 1}$ is listed at ENDL at 17.128 keV, and at 17.222 keV at LBNL. The resulting systematic error can make the correct identification of lines difficult, e. g. for the observed line at (nominally) 17.8 keV. It can also make it difficult to distinguish potential non-linearities in the detector response from systematic errors in the energy calibration. The existence of these errors is likely due to the fact that the low energy region has not been used much for γ-analysis with Ge detectors. The availability of better detectors now increases the need for better low-energy calibration lines to fully exploit the rich spectral structure of the very low energy region. In addition, the new data bases should also include the branching ratios for very low γ-emissions (which are often not listed at LBNL or BNL), to assess their contribution to the spectra and their potential use for NDA.

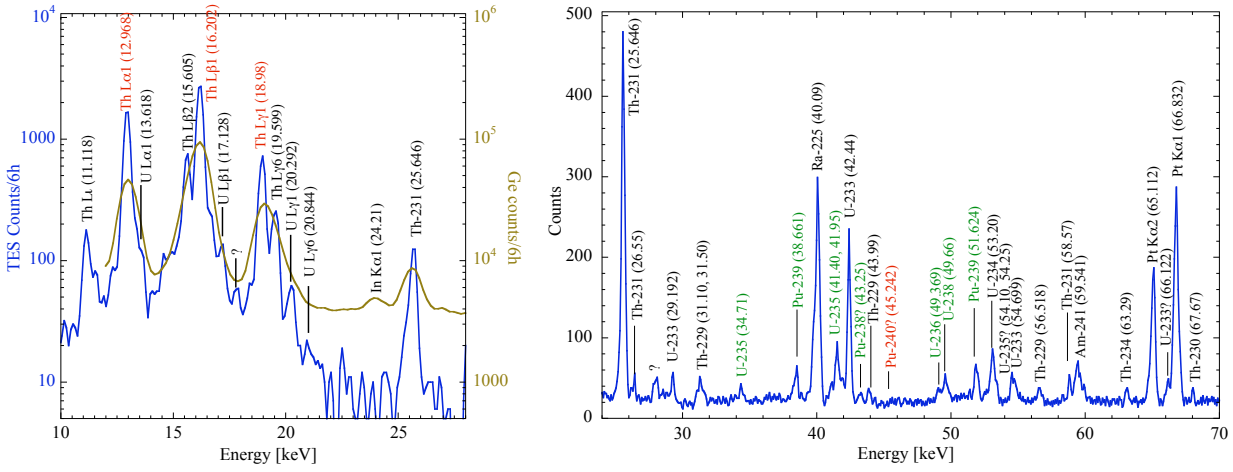

Figure 3 (left): Low-energy response of the TES γ-detector to the skull oxide sample, compared to the response of the Ge detector for the same data acquisition time of 6 hours. Figure 4 (right): Four 6-hour TES γ-spectra added for improved statistics. The isotopes labeled in green are not detectable with the Ge detector above the Compton background, even for long acquisition times (cf. figure 2).

A related problem has become apparent as we tried to simulate the low-energy spectrum source output with the Radiation Source ("RadSrc") code. Several lines, e.g. U $L_{\beta 2}$ at 17.128 keV and U $L_{\gamma 6}$ at 20.844 keV, do not appear in the simulated output, presumably because the programmers did not feel the need to include them, as this very low energy region is typically not used for NDA. Programs such as RadSrc should obviously be updated to include these lines.

The additional lines seen in the ultra-high resolution γ-spectrum demonstrate that TES detectors can detect isotopes whose emissions are overshadowed either by neighboring lines or by the Compton background when using a Ge detector. For example, the skull oxide contains mostly U isotopes, but since it is derived form reprocessed material, it contains small amounts of Pu. However, the strongest Pu emission lines are the U L X-rays, which cannot be resolved with Ge detectors because they lie in the wings of the Th L X-rays from the U decay. Superconducting detectors allow non-destructive measurements of the Pu activity even for high U concentrations.

Figure 4 illustrates the second advantage of superconducting detectors, namely an improved peak-to-background ratio P/B compared to Ge detectors. At the Th-231 line at 25 keV, the P/B for TES γ-detectors exceeds 30, an order of magnitude higher than for the Ge detector (figure 3), because the intrinsically small size of the TES reduces the Compton contribution form high-energy emission lines. This allows detecting comparably weak lines despite only moderate statistics. Specifically, it allows detecting the weak γ-emissions from Pu-238 at 42.25 keV, and the Pu-239 at 38.661 and 51.624 keV. So far, the Pu-240 line at 45.242 keV is still not detectable when adding four 6-hour TES spectra. The P/B ratio for superconducting TES detectors is even higher for the L X-ray region below 20 keV.

The detection of the characteristic emission from U isotopes allows a non-destructive estimate of the U isotopic composition. The measured 235:233 intensity ratio in the 40 keV region is 98:193. For branching ratios of 0.0862 for the U-233 line at 42.41 keV and 0.09 for the sum of the two U-235 lines at 41.4 and 41.95 keV, the atomic ratio of U-233 and U-235 is given by

$$\frac{(233)}{(235)} = \frac{193 \cdot 1.592 \cdot 10^5}{0.0862} \frac{0.09}{98 \cdot 7.038 \cdot 10^8} \approx 0.05\%$$

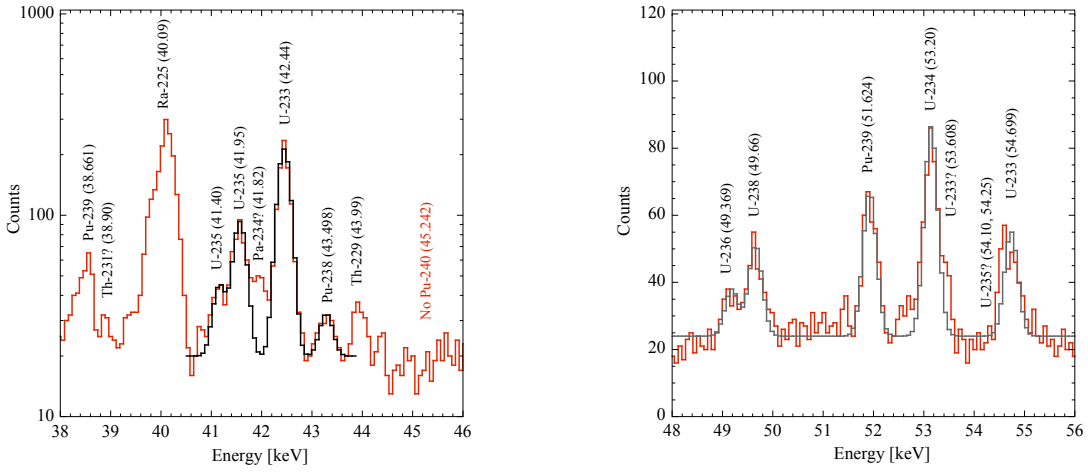

Figure 5 (left): 40 keV region of the spectrum in figure 4 with a Gaussian fit to four of the actinide emission lines. Figure 6 (right): 50 keV region with a Gaussian fit to five of the actinide emission lines. This region contains γ-rays from all major uranium isotopes, U-233, U234, U-235, U-236 and U-238, in close vicinity, and can therefore be used for quantitative high-precision uranium isotope ratio measurements.

This is significantly less that the ICP-MS analysis at SRNL, and suggests major systematic errors. At present, the error bar on measurements that we can account for is on the order of ±25%. It is dominated by systematic errors form background subtraction and non-Gaussian line shapes for the strong γ-lines and statistics for the weaker lines. In addition, the systematic errors in the branching ratios are significant. For example, according to the LBNL table of isotopes, the U-235 lines at 41.4 and 41.95 keV have nominal branching ratios of 0.03(2) and 0.06(1). However, the measured intensity ratio is about 1:3, implying a systematic error of at least 25%. The total error will likely be reduced when the entire spectral region with all lines up to 200 keV is used for the analysis, but so far the low-energy branching ratios have not been determined with sufficient precision for good quantitative analysis. This will be the focus of future work.

A more precise quantitative analysis of the spectra also requires a better calibration of the detector efficiency. This quantification will also benefit from a better knowledge of the low-energy ranching ratios, which also vary considerably in the literature. Low error bars on the branching ratios of the U L X-rays for different Pu isotopes could, for example, be used to extract Pu isotopics from these X-rays below 20 keV.

In summary, the low-energy region of γ-/ X-ray spectra is rich in information because of the multitude of lines. So far, most NDA does not use this region because Ge detectors do not have the resolution to separate the individual lines and typically have too high a Compton background. Superconducting detectors change this game, since their ultra-high energy resolution and improved peak-to-background ratio makes the so far unexploited low-energy region resolvable. We have demonstrated that different U and Pu γ-emissions can be detected with superconducting spectrometers that were obscured by line overlap or the Compton background when using Ge detectors. This increases the precision of NDA of nuclear materials, including weakly radioactive samples and reprocessed fuel samples.

Conclusions: • Superconducting TES γ-detectors allow NDA of nuclear materials at (so far unused) low energies where the actinide emissions with highest intensity lie.

- They can detect γ-emission lines that were obscured when using Ge detectors and can thus increase the sensitivity for NDA of weakly radioactive samples.
- Characterization of the response function and improved measurements of γ-energies and branching ratios will enable quantitative analysis.
- Improved uniformity of the detector response is necessary for good Gaussian line shapes
- Simulations need to be updated to include all low-energy emissions lines.
- Variations by up to ±100 eV in tabulated line energies cause systematic calibration errors.

Superconducting TES detectors offer a powerful improvement to NDA, but more work needs to be done to fully exploit their potential benefits, especially at very low energy. We are currently preparing a more detailed analysis of this sample for publication in the open literature.

Acknowledgements: This work was supported by the U.S. DOE, Office of Nuclear Energy under grant LL0915040309. It was performed under the auspices of the U.S. Department of Energy by Lawrence Livermore National Laboratory under Contract DE-AC52-07NA27344.